

A Comprehensive Study of Multimodal Large Language Models for Image Quality Assessment

Tianhe Wu^{1,2}, Kede Ma^{2*}, Jie Liang³, Yujiu Yang^{1*}, and Lei Zhang^{3,4}

¹ Shenzhen International Graduate School, Tsinghua University

² Department of Computer Science, City University of Hong Kong

³ OPPO Research Institute

⁴ The Hong Kong Polytechnic University

wth22@mails.tsinghua.edu.cn, kede.ma@cityu.edu.hk, liang27jie@gmail.com,

yang.yujiu@sz.tsinghua.edu.cn, cslzhang@comp.polyu.edu.hk

<https://github.com/TianheWu/MLLMs-for-IQA>

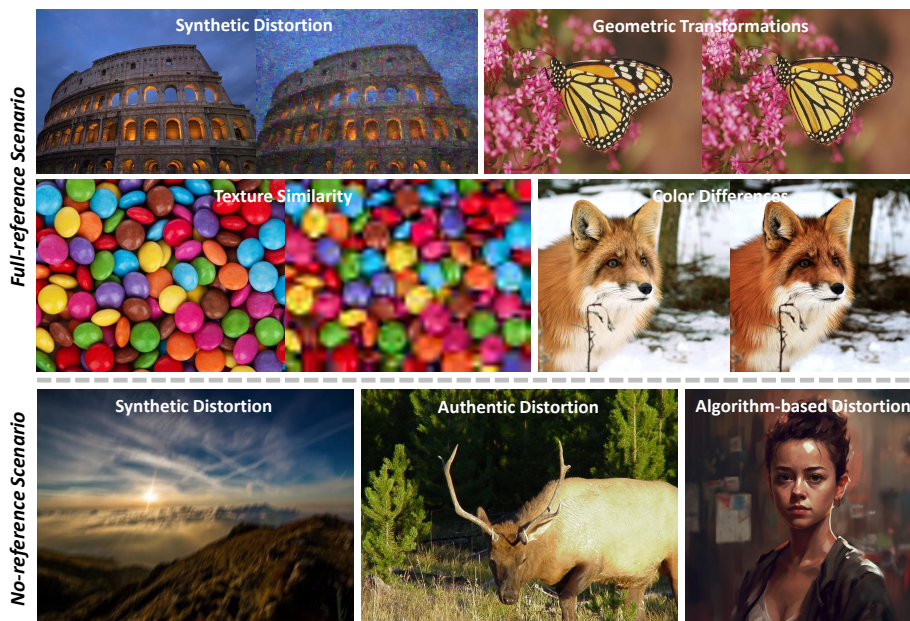


Fig. 1: Illustration of several visual attributes of image quality in our experiments.

Abstract. While Multimodal Large Language Models (MLLMs) have experienced significant advancement on visual understanding and reasoning, their potentials to serve as powerful, flexible, interpretable, and text-driven models for Image Quality Assessment (IQA) remains largely unexplored. In this paper, we conduct a comprehensive and systematic study of prompting MLLMs for IQA. Specifically, we first investigate nine prompting systems for MLLMs as the combinations of three standardized testing procedures in psychophysics (*i.e.*, the single-stimulus, double-stimulus, and multiple-stimulus methods) and three popular prompting

* Corresponding author.

strategies in natural language processing (*i.e.*, the standard, in-context, and chain-of-thought prompting). We then present a difficult sample selection procedure, taking into account sample diversity and uncertainty, to further challenge MLLMs equipped with the respective optimal prompting systems. We assess three open-source and one close-source MLLMs on several visual attributes of image quality (*e.g.*, structural and textural distortions, color differences, and geometric transformations) in both full-reference and no-reference scenarios. Experimental results show that only the close-source GPT-4V provides a reasonable account for human perception of image quality, but is weak at discriminating fine-grained quality variations (*e.g.*, color differences) and at comparing visual quality of multiple images, tasks humans can perform effortlessly.

Keywords: Image quality assessment · Multimodal large language models · Model benchmarking

1 Introduction

The evolution of Large Language Models (LLMs) has marked a significant milestone in the field of Artificial Intelligence (AI) [2, 6, 49, 53]. The underlying idea of scaling the model size and training data [20] has rendered LLMs the abilities to perform various Natural Language Processing (NLP) tasks with unprecedented levels of accuracy [2].

In the midst of these developments, a particularly promising offshoot has emerged in the form of Multimodal LLMs (MLLMs). These advanced models have taken the capabilities of LLMs a step further by incorporating visual data alongside text [4, 13, 31, 46, 61, 64]. MLLMs typically integrate visual data via Vision Transformers (ViTs) [14] for feature extraction, attention mechanisms [50] for visual-textual relationship modeling, and fusion modules [3, 17, 26] to merge the two modalities. These techniques enable MLLMs to process both text and image data holistically, extending the application scenario of LLMs.

Apart from their high-level visual understanding and reasoning capabilities [31, 61], MLLMs also open up substantial opportunities for Image Quality Assessment (IQA) [52]. As a fundamental vision task, IQA aims to devise computational models to predict image quality as perceived by the Human Visual System (HVS). Ideally MLLMs shall benefit IQA in the following aspects.

- **Improved accuracy.** MLLMs are commonly built upon strong visual encoders [32, 42], which are exposed to massive images of various vision tasks closely related to (and including) IQA. This allows MLLMs to cross-validate visual information from different vision tasks for improved IQA, which is in a similar spirit to multitask learning for IQA [35, 71].
- **Improved robustness.** Being *sequential* in nature, MLLMs do not rely on alignment of images for quality assessment, making them easily robust to perturbations that are imperceptible to the human eye, such as mild geometrical transformations [34] and texture substitution [11].

- **Flexibility.** Text as one modality of input, MLLMs enable a wide range of text-conditioned IQA, for example, IQA for semantically meaningful local regions [66], fine-grained visual attributes (*e.g.*, color appearance and well-exposedness) [9], and various viewing conditions and display systems [10].
- **Interpretability.** MLLMs generate descriptive text rather than merely providing a numerical score [67]. This text output allows for more detailed, contextually rich, and human-like quality assessment, making MLLMs valuable for IQA model-in-the-loop image enhancement [29].

Previous work [55, 56, 67] focuses primarily on establishing IQA datasets with human quality descriptions to benchmark MLLMs in terms of quality question answering, rating, and reasoning. Appealing at first glance, these studies may suffer from several limitations. First, how to properly instruct human subjects to supply detailed and balanced descriptions of image quality and other relevant visual information is highly nontrivial. Second, image quality is a perceptual quantity with subjective biases. How to screen outlier descriptions and aggregate valid but relatively inconsistent descriptions are overlooked. Third, comparing MLLM outputs to reference descriptions is complex, and remains an intriguing and challenging problem in language modeling [1, 28]. After all, the field of IQA has a rich history, and numerous established human-rated image quality datasets are readily accessible for evaluating this perceptual aspect of MLLMs. Closest to ours, Zhu *et al.* [73] tested the pairwise quality comparison capability of MLLMs in a constrained context.

In this work, we further pursue this direction, and conduct a comprehensive and systematic study of prompting MLLMs for IQA, as opposed to optimizing individual text prompts. We first explore nine prompting systems for MLLMs, combining standardized testing procedures in psychophysics (*i.e.*, the single-stimulus, double-stimulus, and multiple-stimulus methods) with popular prompting strategies in NLP (*i.e.*, the standard, in-context, and chain-of-thought prompting). Interestingly, we discover that the optimal prompting system varies between open-source [13, 31, 64] and closed-source MLLMs. To further challenge MLLMs, we propose a computational procedure to select difficult samples using top-performing IQA expert models as proxies [8, 11, 57, 60, 69, 71], while taking into account sample diversity and uncertainty. Under both Full-Reference (FR) and No-Reference (NR) settings, we experiment with three open-source and one close-source MLLMs across several visual attributes of image quality, including structural and textural distortions, color differences, and geometric transformations (see Fig. 1). Experimental results show that even the most advanced MLLM (*i.e.*, the proprietary GPT-4V) still has room for improvement in modeling the incredibly sophisticated adaptable HVS for IQA.

2 Related Work

In this section, we present a summary of expert models and MLLMs for IQA.

2.1 Expert Models for IQA

IQA can be roughly divided into two categories: FR- and NR-IQA. FR-IQA models are preferred in situations where the unimpaired reference image is available, such as in many low-level vision tasks. Representative design philosophies for FR-IQA range from measuring error visibility (*e.g.*, the mean squared error (MSE)), structural similarity (*e.g.*, the SSIM index [52]), and mutual information (*e.g.*, the VIF measure [43]) to (deep) learning-based methods (*e.g.*, the LPIPS [69] and DISTs metrics [11]) and fusion-based approaches (*e.g.*, VMAF [48]). Almost all FR-IQA models depend on the proper alignment of the reference and test images to execute co-located comparison at the pixel, patch, or feature level. Consequently, these models may struggle to capture the robustness of the HVS to mild geometric transformations and texture resampling. Additionally, these models frequently disregard or give a superficial treatment of color information, leading to a poor account for perceptual color differences [9, 51].

NR-IQA models [21, 37, 59, 60, 63, 70, 71] are the most challenging yet widely applicable as they are designed to evaluate image quality without any reference. Regardless of whether they are knowledge-driven [37] or data-driven [70, 71], NR-IQA models rely heavily on the training data, which often demonstrate weak generalization when faced with a broader type of images and distortions.

Apart from accuracy and generalization, expert IQA models also fall short in terms of flexibility and interpretability. This is primarily because they reduce the evaluation of image quality to a numerical score, failing to leverage other formats of inputs, and output other detailed and perceptually relevant information.

2.2 MLLMs for IQA

Previous work has been centered on benchmarking and refining MLLMs for IQA. The pioneering datasets, DepictQA [67] and Q-Bench [55], have initiated the assessment of MLLMs in quality rating and reasoning under the FR and NR conditions, respectively. DepictQA employs a double-stimulus method, prompting MLLMs to compare a pair of images against a standard reference. In contrast, Q-Bench takes a single-stimulus approach, assigning a numerical score based on the classification of image quality as “poor” or “good”. Notably, these investigations reveal that, except for the proprietary GPT-4V [61], open-source MLLMs like LLaVA [31], Kosmos-2 [41], and MiniGPT-4 [72] show limited success in replicating human perception of image quality. Efforts to enhance open-source MLLMs through instruction tuning have been made [56], focusing on the prediction of subsequent tokens. Yet, such models often revert to generating template-like quality descriptions, lacking the level of flexibility we are looking for. In this work, we take a step back and conduct a comprehensive and systematic exploration of prompting techniques for MLLMs on existing human-rated IQA datasets.

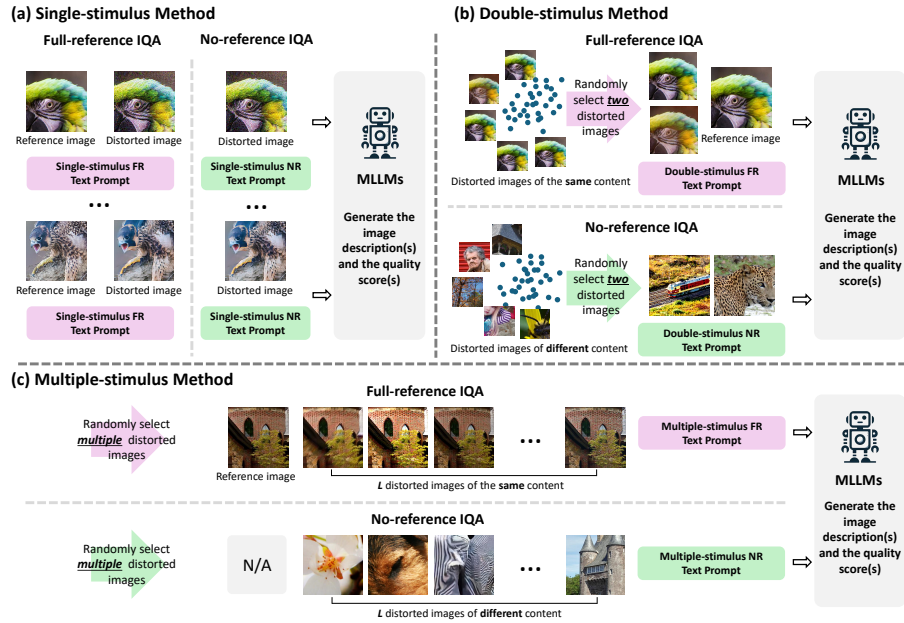


Fig. 2: Three standardized psychophysical testing procedures for IQA. (a) Single-stimulus method. (b) Double-stimulus method. (c) Multiple-stimulus method.

3 Systematic Prompting MLLMs for IQA

In this section, we introduce several prompting systems for MLLMs in the context of IQA, followed by describing the difficult sample selection procedure.

3.1 Systematic Prompting from Psychophysics

Although MLLMs and the HVS (or more generally the human brain) operate in different domains, they have fascinating similarities, especially in representational hierarchy [5], visual-textual integration, contextual reasoning [22], and adaptation [12]. Thus, it is natural to employ standardized psychophysical testing procedures as the systematic prompting methods for IQA.

Single-stimulus Method. As depicted in Fig. 2 (a), given a test image $x \in \mathcal{X}$, the FR single-stimulus method⁵ suggests MLLMs to output a quality score, $q(x) \in [0, 100]$, based on its perceptual difference to the corresponding reference image $y \in \mathcal{Y}$. Here, a larger number indicates higher quality. In contrast, the NR single-stimulus method derives the quality score solely from the perceptually important visual attributes of the test image x . Generally, the single-stimulus method is scalable and straightforward to implement for MLLMs, but may not

⁵ This is also known as the double-stimulus impairment rating by treating the reference image as a second visual stimulus.

capture relative quality accurately and may exhibit context dependency (*e.g.*, the presentation order).

Double-stimulus Method. Also known as two-alternative forced choice (2AFC) and paired comparison, the double-stimulus method first samples a pair of images either uniformly or actively [62] from a set of images $\mathcal{X} = \{x_i\}_{i=1}^M$, where M is the number of images. In our implementation, MLLMs are not forced to select between the two alternatives with higher quality. Instead, they have a third option: the quality of the two images is comparable. Fig. 2 (b) illustrates the FR and NR double-stimulus methods. In the FR scenario, the pair of images are constrained to share the same underlying visual content but differ in types and intensities of distortions. Additionally, a reference image is supplied to facilitate quality comparison. In the NR scenario, the pair of images can be of different content, without supplying any reference image. Upon constructing the pairwise preference matrix $C \in \mathbb{R}^{M \times M}$, where

$$C_{ij} = \begin{cases} \# \text{ times } x_i \text{ preferred over } x_j & \text{if } i \neq j \\ 0 & \text{if } i = j, \end{cases} \quad (1)$$

we adopt the maximum a posteriori estimation to aggregate pairwise rankings, under the Thurstone’s Case V assumption [47]. This amounts to solving the following convex optimization problem:

$$\begin{aligned} \arg \max_{\mu} \quad & \sum_{i,j} C_{ij} \log(\Phi(\mu_i - \mu_j)) - \sum_i \frac{\mu_i^2}{2} \\ \text{subject to} \quad & \sum_i \mu_i = 0, \end{aligned} \quad (2)$$

where $\mu = [\mu_1, \mu_2, \dots, \mu_M]$ are the global quality scores for the M images and $\Phi(\cdot)$ is the standard normal cumulative distribution function. Alternative pairwise ranking aggregation methods can be employed, such as the Thurstone-Mosteller least squares, the Perron-Frobenius ranking, and the ELO system [15]. We find empirically that these approaches all yield reliable and consistent ranking outcomes. Arguably the double-stimulus method is considered more reliable than the single-stimulus counterpart when gathering human opinions of image quality, despite its $O(M^2)$ sample complexity. It remains to be seen whether such reliability extends to prompting MLLMs.

Multiple-stimulus Method. As shown in Fig. 2 (c), the multiple-stimulus method proposes a more efficient approach to gather partial rankings by simultaneously presenting a set of L images to MLLMs for ranking. Just like the double-stimulus method, in the FR scenario, we limit the list of L images to have identical visual content and supply the corresponding reference image. This restriction and the presence of the reference image are not assumed in the NR scenario. The listwise ranking of L images yields $\binom{L}{2}$ pairwise rankings, which are used to form the pairwise preference matrix C in Eq. (1), followed by ranking aggregation using Eq. (2).

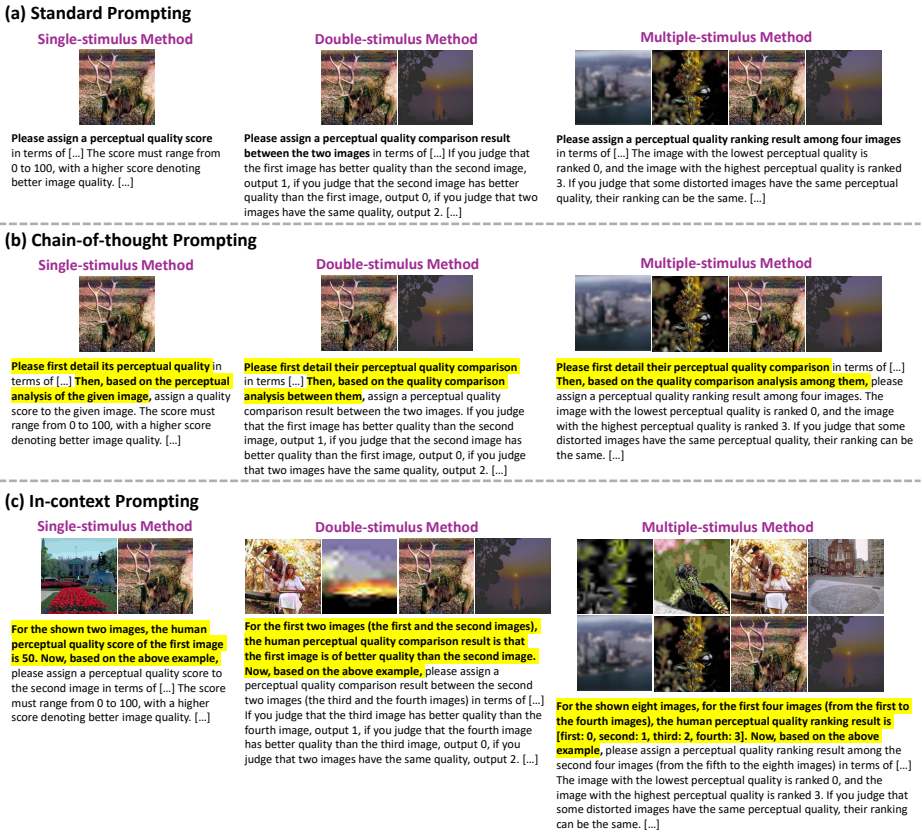


Fig. 3: Instantiations of systematic prompting strategies for GPT-4V in the NR scenario. (a) Standard prompting. (b) Chain-of-thought prompting. (c) In-context prompting. See complete FR and NR text prompts in the supplementary material.

Fig. 3 gives the detailed text prompts to implement the single-stimulus, double-stimulus and multiple-stimulus methods for GPT-4V in the NR-IQA scenario. It is crucial to acknowledge that our priority is not to optimize individual textual prompts at the token level, but to explore the impact systematic prompting methods on IQA.

3.2 Systematic Prompting from NLP

MLLMs evolve from LLMs, thereby inherently accommodating systematic prompting strategies in NLP.

Standard Prompting. As shown in Fig. 3 (a), the standard (and the most basic) prompting method is to directly query the quality score, comparison and ranking results without any exemplars [44] nor descriptions to elicit intermediate reasoning steps. This type of prompting is characterized by its brevity, which has been used in [73] to implement the double-stimulus method.

Chain-of-thought Prompting. As a simple yet powerful approach to encouraging step-by-step reasoning, chain-of-thought prompting [54] has proven to be highly beneficial for a range of NLP tasks. In the same vein, we request MLLMs to detail the perceptual quality of the test image(s) by examining various visual attributes (and comparing to the reference image(s) when available), before integrating the analysis results into overall quality estimate(s) (see Fig. 3 (b)).

In-context Prompting. One of the key breakthroughs of LLMs is their ability to perform in-context (*i.e.*, few-shot) prompting [65]. By incorporating just a handful of exemplars during inference, LLMs are adept at making accurate predictions, even on tasks they have not encountered before. Such ability to adapt without additional training is particularly valuable and worth investigating for MLLMs. Thus, as depicted in Fig. 3 (c), we apply the in-context prompting method by demonstrating MLLMs image(s) with human quality score(s). Subsequently, we ask MLLMs to assess the quality of the test image(s).

By integrating prompting strategies derived from psychophysics and NLP, we end up with nine prospective prompting systems for testing. Given the variations in model architectures, training data, optimization pipelines, and alignment paradigms [38, 39, 74], it is anticipated that different MLLMs may function optimally with different prompting systems.

3.3 Computational Procedure for Difficult Sample Selection

Inference with MLLMs tends to be slow and costly, making it impractical to evaluate MLLMs on the full IQA datasets paired with the proposed nine prompting systems. We describe a computational procedure to pinpoint a smaller set of the most informative samples that meet three key criteria.

First, they should be *difficult*, with a high likelihood of causing MLLMs to err. The Group MAXimum Differentiation (gMAD) competition [36] has been used before for difficult sample selection, but it is not applicable here due to the violation of affordable inference assumption. We thus utilize efficient expert IQA models as proxies, and identify their failures by maximizing the MSE between model predictions and human quality scores, as a form of “black-box” attacks [40] on MLLMs. Second, the selected samples should be *diverse* to highlight various aspects of MLLMs’ potential weaknesses in IQA. Third, they should be *consistent* with small variations in individual quality scores. That is, samples that have inconsistent or uncertain human ratings are less meaningful to assess MLLMs. Putting together, we have the following optimization problem in the FR scenario:

$$y_n^* = \operatorname{argmax}_{y \in \mathcal{Y} \setminus \mathcal{Y}_{n-1}^*} \frac{1}{|\mathcal{X}_y|} \sum_{x \in \mathcal{X}_y} \frac{(d_w(x, y) - q(x))^2}{(\sigma(x))^2 + \epsilon} + \lambda \operatorname{Div}(y, \mathcal{Y}_{n-1}^*), \quad (3)$$

where $\mathcal{Y}_{n-1}^* = \{y_{n'}^*\}_{n'=1}^{n-1}$ contains the selected reference images in the previous $n - 1$ iterations from \mathcal{Y} , the set of all reference images. \mathcal{X}_y includes all distorted images that originate from y . $d_w(\cdot, \cdot)$ denotes the expert FR-IQA model, parameterized by w . $q(\cdot)$ and $\sigma(\cdot)$ are respectively the human quality score and standard deviation. $\operatorname{Div}(\cdot)$ is the point-to-set measure, quantifying the added diversity of

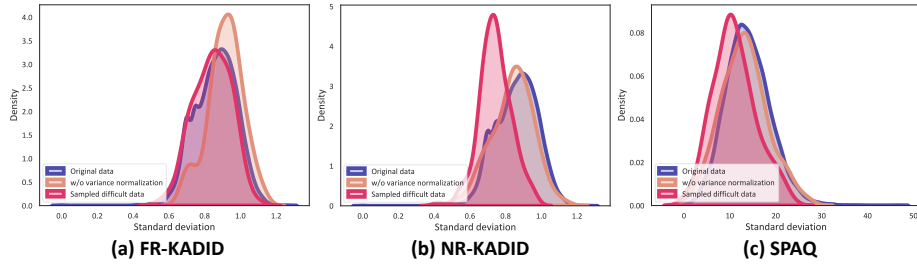


Fig. 4: Comparison between difficult sample selection with and without variance normalization under the same level of sample diversity.

y to \mathcal{Y}_{n-1}^* . λ is a parameter, trading off the variance-normalized squared error and the diversity measure. ϵ is a small positive constant to avoid any potential division by zero.

For each of the N identified reference images, we sample top- K difficult distorted images by solving

$$x_k^* = \operatorname{argmax}_{x \in \mathcal{X}_y \setminus \mathcal{X}_{k-1}^*} \frac{(d_w(x, y) - q(x))^2}{(\sigma(x))^2 + \epsilon}, \quad y \in \mathcal{Y}_N^*, \quad (4)$$

where $\mathcal{X}_{k-1}^* = \{x_{k'}^*\}_{k'=1}^{k-1}$. Similarly, in the NR scenario, we sample top- N difficult images by slightly modifying Eq. (3):

$$x_n^* = \operatorname{argmax}_{x \in \mathcal{X} \setminus \mathcal{X}_{n-1}^*} \frac{(q_w(x) - q(x))^2}{(\sigma(x))^2 + \epsilon} + \lambda \operatorname{Div}(x, \mathcal{X}_{n-1}^*), \quad (5)$$

where $q_w(\cdot)$ denotes the expert NR-IQA model. Fig. 4 shows the comparison between difficult sample selection with and without variance normalization (as a measure of sample uncertainty) under the same level of sample diversity. We find that variance-normalized sampling induces a noticeable shift towards zero in the empirical distribution of sample standard deviations, suggesting an enhanced level of human consistency in assessing image quality.

4 Experiments

In this section, we commence by presenting the experimental setups, and subsequently undertake a comprehensive evaluation of the nine prompting systems.

4.1 Experimental Setups

Datasets. We examine four visual attributes in the FR scenario, including synthetic structural and textural distortions, texture similarity, color differences, and geometric transformations. The selected datasets are FR-KADID [30],

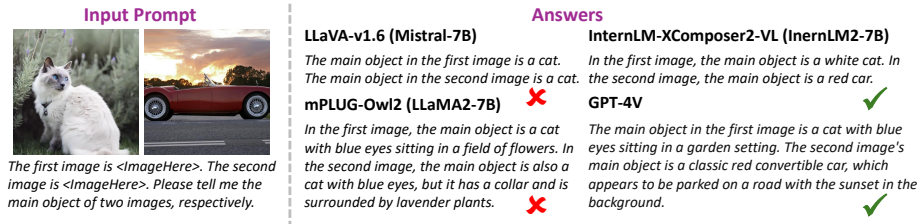


Fig. 5: Behaviors of different MLLMs in recognizing objects from multiple images.

TQD [11], SPCD [51], and Aug-KADID⁶ [30], respectively. In the NR scenario, we examine synthetic and authentic structural and textual distortions and algorithm-based artifacts, using the NR-KADID [30], SPAQ [16], and AGIQA-3K [25] datasets, respectively.

Sample Selection Details. In the FR scenario, the numbers of sampled reference images N and the corresponding distorted images K are set to 15 and 10, respectively. In the NR scenario, the number of selected images N is set to 150. The trade-off parameter λ and the stability constant ϵ in Eqs. (3) and (5) are set to 0.01 and 1, respectively. The point-to-set diversity measure $\text{Div}(\cdot)$ is implemented by the MSE in the feature space of the CLIP visual encoder [42]. The expert FR-IQA model $d_w(\cdot, \cdot)$ and the expert NR-IQA model $q_w(\cdot)$ are linearly fused with equal weightings using two top-performing models - one excelling in maintaining within-dataset correlation, and the other demonstrating robust cross-dataset generalization. Specifically, for within-dataset performance, we select TOPIQ [8] on FR-KADID [30], DISTS [11] on TQD [11] and Aug-KADID [30], CDNet [51] on SPCD [51], LIQE [71] on SPAQ [16] and NR-KADID [30], and Q-Align [57] on AGIQA-3K [25]. For cross-dataset performance, we choose LPIPS [69] and MANIQA [60] in the FR and NR scenarios, respectively.

4.2 Comparison of Nine Prompting Systems

We initially combine the nine prompting systems with three open-source MLLMs: LLaVA-v1.6 (Mistral-7B) [31], InternLM-XComposer2-VL (InternLM2-7B) [13] and mPLUG-Owl2 (LLaMA2-7B) [64] and one close-source MLLM: GPT-4V [61], and compare them on 150 *uniformly sampled* images, with the goal of identifying the best prompting system for each MLLM. Table 1 shows the Spearman’s rank correlation coefficient (SRCC) results.

Analysis of the Two IQA Scenarios. From the Table, it is evident that no open-source MLLMs achieve satisfactory IQA results in the FR scenario regardless of the prompting system used. These models may generate irrelevant text outputs or encounter complete failures when the input text prompts become more detailed and elaborate. We hypothesize that these models are predominantly trained or aligned on single-image vision tasks, making them struggle with analyzing multiple images, especially of the same underlying content [31]. Fig. 5

⁶ We follow [11] to introduce mild geometric transformations.

Table 1: SRCC results of MLLMs paired with different prompting systems on uniformly sampled images. Model-S, Model-I, and Model-C denote the standard prompting, in-context prompting, and chain-of-thought prompting, respectively. The best result in each section is highlighted in bold.

Method	FR IQA				NR IQA		
	FR-KADID	Aug-KADID	TQD	SPCD	NR-KADID	SPAQ	AGIQA-3K
Single-stimulus				Method			
LLaVA-v1.6-S	0.227	0.013	0.180	0.001	0.262	0.544	0.614
mPLUG-Owl2-S	0.285	0.218	0.228	0.081	0.126	0.467	0.279
InternLM-XC2-VL-S	0.274	0.272	0.299	0.009	0.252	0.794	0.512
GPT-4V-S	0.745	0.786	0.773	0.098	0.467	0.860	0.420
LLaVA-v1.6-I	0.249	0.194	0.222	0.147	0.116	0.019	0.061
mPLUG-Owl2-I	0.373	0.373	0.246	0.047	0.017	0.083	0.409
InternLM-XC2-VL-I	0.380	0.241	0.204	0.087	0.188	0.342	0.461
GPT-4V-I	0.771	0.753	0.738	0.028	0.590	0.845	0.650
LLaVA-v1.6-C	0.164	0.300	0.226	0.174	0.151	0.550	0.580
mPLUG-Owl2-C	0.387	0.361	0.278	0.122	0.179	0.455	0.409
InternLM-XC2-VL-C	0.237	0.306	0.167	0.063	0.306	0.649	0.507
GPT-4V-C	0.809	0.782	0.809	0.121	0.517	0.869	0.677
Double-stimulus				Method			
LLaVA-v1.6-S	0.387	0.396	0.390	0.113	0.270	0.430	0.234
mPLUG-Owl2-S	0.435	0.307	0.350	0.117	0.126	0.157	0.020
InternLM-XC2-VL-S	0.309	0.408	0.440	0.042	0.267	0.690	0.555
GPT-4V-S	0.679	0.743	0.655	0.031	0.552	0.834	0.599
LLaVA-v1.6-I	0.379	0.396	0.324	0.032	0.169	0.128	0.156
mPLUG-Owl2-I	0.257	0.257	0.169	0.083	0.078	0.164	0.120
InternLM-XC2-VL-I	0.348	0.376	0.379	0.144	0.034	0.108	0.123
GPT-4V-I	0.470	0.244	0.340	0.122	0.531	0.761	0.714
LLaVA-v1.6-C	0.332	0.355	0.257	0.109	0.124	0.065	0.174
mPLUG-Owl2-C	0.409	0.334	0.318	0.013	0.199	0.122	0.130
InternLM-XC2-VL-C	0.332	0.411	0.267	0.131	0.165	0.556	0.546
GPT-4V-C	0.818	0.830	0.786	0.124	0.639	0.881	0.771
Multiple-stimulus				Method			
LLaVA-v1.6-S	0.349	0.351	0.315	0.241	0.169	0.221	0.210
mPLUG-Owl2-S	0.385	0.428	0.297	0.104	0.124	0.061	0.228
InternLM-XC2-VL-S	0.484	0.420	0.241	0.015	0.047	0.044	0.154
GPT-4V-S	0.824	0.844	0.747	0.037	0.397	0.715	0.461
LLaVA-v1.6-I	0.337	0.380	0.356	0.203	0.152	0.033	0.241
mPLUG-Owl2-I	0.268	0.268	0.377	0.067	0.196	0.142	0.121
InternLM-XC2-VL-I	0.489	0.235	0.212	0.046	0.038	0.102	0.114
GPT-4V-I	0.585	0.496	0.389	0.023	0.168	0.416	0.201
LLaVA-v1.6-C	0.292	0.424	0.288	0.043	0.227	0.111	0.122
mPLUG-Owl2-C	0.377	0.406	0.376	0.126	0.214	0.166	0.084
InternLM-XC2-VL-C	0.500	0.466	0.273	0.038	0.031	0.037	0.148
GPT-4V-C	0.761	0.806	0.754	0.036	0.537	0.817	0.679

provides a simple example of how different MLLMs behave when recognizing objects from multiple images, a high-level vision task at which they should excel. However, it appears that LLaVA-v1.6 [31] and mPLUG-Owl2 [64] completely disregard the second image, despite it being explicitly mentioned and separated from the first image in the input prompt. In the NR scenario with single-stimulus standard prompting (*i.e.*, the single-image analysis scenario), LLaVA-v1.6 [31] and mPLUG-Owl2 [64] deliver improved quality prediction accuracy. Moreover, InternLM-XComposer2-VL [13] and GPT-4V perform remarkably in handling realistic camera distortions on SPAQ [16].

Analysis of Psychophysical Prompting Methods. The results in the table reveal that for the three open-source MLLMs, the single-stimulus method is the optimal choice due to their limited ability to analyze multiple images. In stark contrast, GPT-4V [61] benefits from multiple-image analysis, and per-

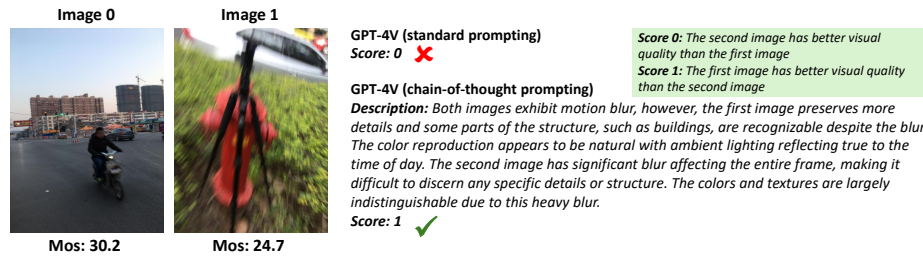


Fig. 6: Comparison of the double-stimulus standard and chain-of-thought promptings for GPT-4V in the NR scenario.

forms optimally under the double-stimulus chain-of-thought prompting. These findings raise questions about recent claims [58] that open-source MLLMs have surpassed GPT-4V-level IQA performance by instruction tuning on existing (weakly-)annotated benchmarks, given that the optimal prompting system has not been paired with GPT-4V.

Analysis of NLP Prompting Methods. It is expected that in-context prompting is little likely to bring performance gains to the three open-source MLLMs due to the added complexity of processing additional image(s) in the context. Interestingly, we find that in-context prompting does not aid GPT-4V with the single-stimulus prompting. When combined with the multiple-stimulus prompting, GPT-4V performs poorly across various visual attributes and in both the FR and NR scenarios. To take a closer look, we compare the single-stimulus in-context prompting with double-stimulus standard prompting for GPT-4V. The main difference is that the former offers a human quality score for the contextual image, aiming to aid visual quality comparison. The comparable performance achieved by both prompting systems suggests that the inclusion of a human quality score has minimal impact on the GPT-4V inference. In cases when the input prompt contains a large number of images (*e.g.*, eight images for the multiple-stimulus in-context prompting), even GPT-4V finds difficult in processing such substantial amount of visual information, resulting in a sharp drop in prediction accuracy.

The chain-of-thought prompting, on the other hand, paints a different picture: it consistently enhances the performance of GPT-4V [61] in conjunction with three psychophysical testing protocols and across nearly all visual attributes. The remarkable improvements may arise because the chain-of-thought prompting elicits the break down of the intricate IQA task into simpler sub-tasks. This allows for a more meticulous inspection of visually critical factors such as structure and texture preservation, as well as color and luminance reproduction. On the other hand, as shown in Fig. 6, the chain-of-thought prompting encourages absorbing IQA into a boarder and higher-level task, orchestrating with additional physical, geometrical, and semantic information of the natural scene to infer image quality. This reminds the authors of a famous slogan in computer vision: “If you cannot solve a simple problem in vision, you may have to solve a complex one (by Songchun Zhu)”.

Table 2: Comparison of MLLMs with optimally suited prompting systems against expert IQA systems in the FR scenario. Black and blue numbers in bold represent the best expert IQA systems and the MLLMs, respectively. * indicates that the model has been trained on the dataset.

Method	FR-KADID		Aug-KADID		TQD		SPCD	
	SRCC	PLCC	SRCC	PLCC	SRCC	PLCC	SRCC	PLCC
PSNR	0.479	0.675	0.381	0.644	0.345	0.522	0.576	0.570
SSIM [52]	0.553	0.694	0.405	0.633	0.510	0.618	0.229	0.246
FSIM [68]	0.704	0.762	0.400	0.560	0.332	0.408	0.205	0.206
LPIPS [69]	0.477	0.654	0.547	0.654	0.469	0.511	0.280	0.252
AHIQ [24]	0.512	0.583	0.512	0.688	0.467	0.608	0.240	0.269
DISTS [11]	0.647*	0.740*	0.701	0.696	0.911	0.901	0.454	0.422
LLaVA-v1.6 [31]	0.112	0.218	0.198	0.213	0.180	0.226	0.037	0.008
mPLUG-Owl2 [64]	0.248	0.435	0.358	0.484	0.228	0.335	0.102	0.108
InternLM-XC2-VL [13]	0.246	0.336	0.235	0.404	0.299	0.421	0.171	0.143
GPT-4V [61]	0.669	0.795	0.708	0.800	0.786	0.857	0.122	0.234

4.3 Further Testing on Difficult Data

In this subsection, we compare the previous four MLLMs, each with the optimally suited prompting system and a quality-instruction-tuned MLLM, Q-Instruct [56], against representative expert IQA systems, including PSNR, SSIM [52], FSIM [68], LPIPS [69], AHIQ [24] and DISTS [11] as FR models, and NIQE [37], MUSIQ [21], MANIQA [60], LIQE [71] as NR models on the set of difficult data described in Sec. 3.3.

Results in the FR Scenario. Table 2 shows the SRCC and Pearson’s linear correlation coefficient (PLCC) results in the FR scenario. The primary observation is that the selected difficult images by “attacking” expert IQA models using Eqs. (3) and (5) pose a challenge to GPT-4V, with reduced IQA performance. Nevertheless, on FR-KADID with *synthetic structural and textural distortions*, GPT-4V [61] is on par with the leading expert IQA model, FSIM [68], which assesses structural similarity in the feature space. On Aug-KADID and TQD with *geometric transformations* and *texture similarity*, respectively, GPT-4V exhibits a commendable level of resilience, although not as good as DISTS [11]. It is important to recognize that the ways of attaining these aspects of perceptual robustness differ between the two methods. DISTS relies on comparison of spatial averages of VGG [45] feature maps as a complete and holistic texture characterization, whereas GPT-4V benefits from its intrinsic ability to compile and process data sequentially (as highlighted in the Introduction). On SPCD with *color differences*, all MLLMs including GPT-4V encounter challenges in emulating human color perception, and struggle to differentiate images even with clearly noticeable variations in color appearances (to the human eye).

Results in the NR Scenario. Table 3 shows the SRCC and PLCC results in the NR scenario. It is clear that GPT-4V [61] is outstanding in capturing the *authentic structural and textural distortions* on SPAQ, surpassing the two expert IQA systems MUSIQ [21] and LIQE [71]. Notably, the latter has prior exposure to the SPAQ dataset. Furthermore, GPT-4V showcases a remarkable generalizability to AI-generated images, indicating its great potential to guide

Table 3: Comparison of MLLMs with optimally suited prompting systems against expert IQA systems in the NR scenario.

Method	SPAQ		NR-KADID		AGIQA-3K	
	SRCC	PLCC	SRCC	PLCC	SRCC	PLCC
NIQE [37]	0.551	0.616	0.385	0.555	0.610	0.651
MUSIQ [21]	0.769	0.817	0.567	0.653	0.686	0.588
MANIQA [60]	0.546	0.564	0.428	0.387	0.521	0.599
LIQE [71]	0.781*	0.752*	0.866*	0.930*	0.703	0.693
LLaVA-v1.6 [31]	0.317	0.305	0.428	0.370	0.503	0.573
mPLUG-Owl2 [64]	0.270	0.198	0.128	0.187	0.168	0.201
InternLM-XC2-VL [13]	0.580	0.540	0.454	0.361	0.608	0.590
Q-Instruct [56]	0.799*	0.783*	0.635	0.613	0.853*	0.821*
GPT-4V [61]	0.845	0.843	0.513	0.453	0.783	0.746

the optimization of generative AI models for images. Q-Instruct [56], a model fine-tuned from a variant of LLaVA, exhibits significantly enhanced IQA skills compared to LLaVA-v1.6, thus highlighting the effectiveness of visual instruction tuning (particularly on images with similar distortion appearances).

4.4 Discussion and Limitation

We briefly discuss some of the limitations of this work and opportunities for future work. First, the current prompting systems have room for improvement, as the input prompts are not optimized. This presents an opportunity for exploring automatic prompt optimization [18, 27] within our prompting systems. Second, our sampler relies on human quality scores, and is thus only applicable to existing labeled IQA datasets. Extending it to sample from large-scale sets of unlabeled images will need to 1) accelerate the inference speed of MLLMs so as to leverage model falsification methodologies (*e.g.*, the gMAD competition [36]) or 2) train additional failure-prediction modules [7] in a parameter-efficient way [19]. Third, the textual responses produced by MLLMs have not been quantitatively assessed. Prior research has investigated the application of GPT-4 [31] to assess these responses in terms of correctness, consistency, relevance, informativeness, coherence, and naturalness. Given our focus on responses pertinent to visual quality, it seems reasonable to develop a semantic textual similarity model, specifically designed for the IQA task, with improved accuracy and robustness. Fourth, this work does not touch on instruction tuning of MLLMs to enhance the IQA performance. Preliminary efforts have been made by Wu *et al.* [56] and You *et al.* [67] to directly fine-tune open-source MLLMs on datasets with image quality descriptions. Our results suggest a more encouraging approach: incorporating IQA in a boarder vision task for joint optimization, with the goal of achieving an ideal balance between the generality and specificity of pre-trained MLLMs [23, 33, 61].

5 Conclusion

We have presented a comprehensive study of MLLMs for IQA, with emphasis on systematic prompting strategies. Our study arises as a natural combination of

methods from two separate lines of research: psychophysics and NLP. The first involves collecting reliable measurements of perceptual quantities in response to physical stimuli. The second endeavours to design input textual descriptions to an LLM to elicit a specific response. Our experiments have shown that different MLLMs admit different prompting systems to work optimally. This suggests the need for a systematic re-evaluation of the recent progress in MLLMs for IQA, particular in comparison to the state-of-the-art GPT-4V [61]. Moreover, there is still ample room in improving MLLMs (including GPT-4V) for IQA, especially fine-grained quality discrimination and multiple-image quality analysis.

Meanwhile, we have emphasized the importance of sample selection when evaluating MLLMs for IQA, owing to the high cost associated with inference. In response, we have proposed a computational procedure for difficult sample selection, taking into account both sample diversity and uncertainty. Our sampler relies on an inference-efficient expert IQA model, and can be seen as a black box attack on MLLMs, assuming no knowledge of their internal mechanisms nor the external input-output behaviors.

References

1. Achananuparp, P., Hu, X., Shen, X.: The evaluation of sentence similarity measures. In: Data Warehousing and Knowledge Discovery. pp. 305–316 (2008) [3](#)
2. Achiam, J., Adler, S., Agarwal, S., Ahmad, L., Akkaya, I., Aleman, F.L., Almeida, D., Altenschmidt, J., Altman, S., Anadkat, S., et al.: GPT-4 technical report. arXiv preprint arXiv:2303.08774 (2023) [2](#)
3. Alayrac, J.B., Donahue, J., Luc, P., Miech, A., Barr, I., Hasson, Y., Lenc, K., Mensch, A., Millican, K., Reynolds, M., et al.: Flamingo: A visual language model for few-shot learning. In: Advances in Neural Information Processing Systems. vol. 35, pp. 23716–23736 (2022) [2](#)
4. Bai, J., Bai, S., Yang, S., Wang, S., Tan, S., Wang, P., Lin, J., Zhou, C., Zhou, J.: Qwen-VL: A versatile vision-language model for understanding, localization, text reading, and beyond. arXiv preprint arXiv:2308.12966 (2023) [2](#)
5. Bracci, S., Mraz, J., Zeman, A., Leys, G., Op de Beeck, H.: The representational hierarchy in human and artificial visual systems in the presence of object-scene regularities. PLOS Computational Biology **19**(4), 1–5 (2023) [5](#)
6. Brown, T., Mann, B., Ryder, N., Subbiah, M., Kaplan, J.D., Dhariwal, P., Neelakantan, A., Shyam, P., Sastry, G., Askell, A., et al.: Language models are few-shot learners. In: Advances in Neural Information Processing Systems. vol. 33, pp. 1877–1901 (2020) [2](#)
7. Cao, P., Li, D., Ma, K.: Image quality assessment: Integrating model-centric and data-centric approaches. In: Conference on Parsimony and Learning. pp. 529–541 (2024) [14](#)
8. Chen, C., Mo, J., Hou, J., Wu, H., Liao, L., Sun, W., Yan, Q., Lin, W.: TOPIQ: A top-down approach from semantics to distortions for image quality assessment. arXiv preprint arXiv:2308.03060 (2023) [3](#), [10](#)
9. Chen, H., Wang, Z., Yang, Y., Sun, Q., Ma, K.: Learning a deep color difference metric for photographic images. In: IEEE/CVF Conference on Computer Vision and Pattern Recognition. pp. 22242–22251 (2023) [3](#), [4](#)
10. Chubarau, A., Akhavan, T., Yoo, H., Mantiuk, R.K., Clark, J.: Perceptual image quality assessment for various viewing conditions and display systems. In: Image Quality and System Performance. pp. 1–9 (2020) [3](#)
11. Ding, K., Ma, K., Wang, S., Simoncelli, E.P.: Image quality assessment: Unifying structure and texture similarity. IEEE Transactions on Pattern Analysis and Machine Intelligence **44**(5), 2567–2581 (2020) [2](#), [3](#), [4](#), [10](#), [13](#)
12. Dong, Q., Li, L., Dai, D., Zheng, C., Wu, Z., Chang, B., Sun, X., Xu, J., Sui, Z.: A survey for in-context learning. arXiv preprint arXiv:2301.00234 (2022) [5](#)
13. Dong, X., Zhang, P., Zang, Y., Cao, Y., Wang, B., Ouyang, L., Wei, X., Zhang, S., Duan, H., Cao, M., et al.: InternLM-XComposer2: Mastering free-form text-image composition and comprehension in vision-language large model. arXiv preprint arXiv:2401.16420 (2024) [2](#), [3](#), [10](#), [11](#), [13](#), [14](#)
14. Dosovitskiy, A., Beyer, L., Kolesnikov, A., Weissenborn, D., Zhai, X., Unterthiner, T., Dehghani, M., Minderer, M., Heigold, G., Gelly, S., et al.: An image is worth 16x16 words: Transformers for image recognition at scale. In: International Conference on Learning Representations (2020) [2](#)
15. Elo, A.E., Sloan, S.: The rating of chessplayers: Past and present. Arco Pub pp. 1–220 (1978) [6](#)
16. Fang, Y., Zhu, H., Zeng, Y., Ma, K., Wang, Z.: Perceptual quality assessment of smartphone photography. In: IEEE/CVF Conference on Computer Vision and Pattern Recognition. pp. 3677–3686 (2020) [10](#), [11](#)

17. Gao, P., Han, J., Zhang, R., Lin, Z., Geng, S., Zhou, A., Zhang, W., Lu, P., He, C., Yue, X., et al.: LLaMA-Adapter V2: Parameter-efficient visual instruction model. arXiv preprint arXiv:2304.15010 (2023) [2](#)
18. Guo, Q., Wang, R., Guo, J., Li, B., Song, K., Tan, X., Liu, G., Bian, J., Yang, Y.: Connecting large language models with evolutionary algorithms yields powerful prompt optimizers. In: International Conference on Learning Representations (2024) [14](#)
19. Hu, E.J., Shen, Y., Wallis, P., Allen-Zhu, Z., Li, Y., Wang, S., Wang, L., Chen, W.: LoRA: Low-rank adaptation of large language models. In: International Conference on Learning Representations (2022) [14](#)
20. Kaplan, J., McCandlish, S., Henighan, T., Brown, T.B., Chess, B., Child, R., Gray, S., Radford, A., Wu, J., Amodei, D.: Scaling laws for neural language models. arXiv preprint arXiv:2001.08361 (2020) [2](#)
21. Ke, J., Wang, Q., Wang, Y., Milanfar, P., Yang, F.: MUSIQ: Multi-scale image quality transformer. In: IEEE/CVF International Conference on Computer Vision. pp. 5148–5157 (2021) [4](#), [13](#), [14](#)
22. Kewenig, V., Lampinen, A., Nastase, S.A., Edwards, C., DEstalenx, Q.L., Recharadt, A., Skipper, J.L., Vigliocco, G.: Multimodality and attention increase alignment in natural language prediction between humans and computational models. arXiv preprint arXiv:2308.06035 (2024) [5](#)
23. Kotha, S., Springer, J.M., Raghunathan, A.: Understanding catastrophic forgetting in language models via implicit inference. arXiv preprint arXiv:2309.10105 (2023) [14](#)
24. Lao, S., Gong, Y., Shi, S., Yang, S., Wu, T., Wang, J., Xia, W., Yang, Y.: Attentions help CNNs see better: Attention-based hybrid image quality assessment network. In: IEEE/CVF Conference on Computer Vision and Pattern Recognition Workshop. pp. 1140–1149 (2022) [13](#)
25. Li, C., Zhang, Z., Wu, H., Sun, W., Min, X., Liu, X., Zhai, G., Lin, W.: AGIQA-3K: An open database for AI-generated image quality assessment. arXiv preprint arXiv:2306.04717 (2023) [10](#)
26. Li, J., Li, D., Savarese, S., Hoi, S.: BLIP-2: Bootstrapping language-image pre-training with frozen image encoders and large language models. In: International Conference on Machine Learning. pp. 19730–19742 (2023) [2](#)
27. Li, X.L., Liang, P.: Prefix-tuning: Optimizing continuous prompts for generation. In: Association for Computational Linguistics and International Joint Conference on Natural Language Processing. pp. 4582–4597 (2021) [14](#)
28. Li, Y., McLean, D., Bandar, Z.A., O’shea, J.D., Crockett, K.: Sentence similarity based on semantic nets and corpus statistics. IEEE Transactions on Knowledge and Data Engineering **18**(8), 1138–1150 (2006) [3](#)
29. Liang, Z., Li, C., Zhou, S., Feng, R., Loy, C.C.: Iterative prompt learning for unsupervised backlit image enhancement. In: IEEE/CVF International Conference on Computer Vision. pp. 8094–8103 (2023) [3](#)
30. Lin, H., Hosu, V., Saupe, D.: KADID-10k: A large-scale artificially distorted IQA database. In: International Conference on Quality of Multimedia Experience. pp. 1–3 (2019) [9](#), [10](#)
31. Liu, H., Li, C., Wu, Q., Lee, Y.J.: Visual instruction tuning. In: Advances in Neural Information Processing Systems. vol. 36, pp. 1–25 (2024) [2](#), [3](#), [4](#), [10](#), [11](#), [13](#), [14](#)
32. Liu, Z., Lin, Y., Cao, Y., Hu, H., Wei, Y., Zhang, Z., Lin, S., Guo, B.: Swin Transformer: Hierarchical vision transformer using shifted windows. In: IEEE/CVF International Conference on Computer Vision. pp. 10012–10022 (2021) [2](#)

33. Luo, Y., Yang, Z., Meng, F., Li, Y., Zhou, J., Zhang, Y.: An empirical study of catastrophic forgetting in large language models during continual fine-tuning. arXiv preprint arXiv:2308.08747 (2023) [14](#)
34. Ma, K., Duanmu, Z., Wang, Z.: Geometric transformation invariant image quality assessment using convolutional neural networks. In: IEEE International Conference on Acoustics, Speech and Signal Processing. pp. 6732–6736 (2018) [2](#)
35. Ma, K., Liu, W., Zhang, K., Duanmu, Z., Wang, Z., Zuo, W.: End-to-end blind image quality assessment using deep neural networks. IEEE Transactions on Image Processing **27**(3), 1202–1213 (2017) [2](#)
36. Ma, K., Wu, Q., Wang, Z., Duanmu, Z., Yong, H., Li, H., Zhang, L.: Group MAD competition—a new methodology to compare objective image quality models. In: IEEE/CVF Conference on Computer Vision and Pattern Recognition. pp. 1664–1673 (2016) [8](#), [14](#)
37. Mittal, A., Soundararajan, R., Bovik, A.C.: Making a “completely blind” image quality analyzer. IEEE Signal Processing Letters **20**(3), 209–212 (2012) [4](#), [13](#), [14](#)
38. Ngo, R., Chan, L., Mindermann, S.: The alignment problem from a deep learning perspective. In: International Conference on Learning Representations (2022) [8](#)
39. Ouyang, L., Wu, J., Jiang, X., Almeida, D., Wainwright, C., Mishkin, P., Zhang, C., Agarwal, S., Slama, K., Ray, A., et al.: Training language models to follow instructions with human feedback. Advances in Neural Information Processing Systems **35**, 27730–27744 (2022) [8](#)
40. Papernot, N., McDaniel, P., Goodfellow, I., Jha, S., Celik, Z.B., Swami, A.: Practical black-box attacks against machine learning. In: ACM Asia Conference on Computer and Communications Security. pp. 506–519 (2017) [8](#)
41. Peng, Z., Wang, W., Dong, L., Hao, Y., Huang, S., Ma, S., Wei, F.: Kosmos-2: Grounding multimodal large language models to the world. arXiv preprint arXiv:2306.14824 (2023) [4](#)
42. Radford, A., Kim, J.W., Hallacy, C., Ramesh, A., Goh, G., Agarwal, S., Sastry, G., Askell, A., Mishkin, P., Clark, J., et al.: Learning transferable visual models from natural language supervision. In: International Conference on Machine Learning. pp. 8748–8763 (2021) [2](#), [10](#)
43. Sheikh, H.R., Bovik, A.C.: Image information and visual quality. IEEE Transactions on Image Processing **15**(2), 430–444 (2006) [4](#)
44. Shin, S., Lee, S.W., Ahn, H., Kim, S., Kim, H., Kim, B., Cho, K., Lee, G., Park, W., Ha, J.W., et al.: On the effect of pretraining corpora on in-context learning by a large-scale language model. In: The North American Chapter of the Association for Computational Linguistics. pp. 5168–5186 (2022) [7](#)
45. Simonyan, K., Zisserman, A.: Very deep convolutional networks for large-scale image recognition. In: International Conference on Learning Representations (2014) [13](#)
46. Team, G., Anil, R., Borgeaud, S., Wu, Y., Alayrac, J.B., Yu, J., Soricut, R., Schalkwyk, J., Dai, A.M., Hauth, A., et al.: Gemini: A family of highly capable multimodal models. arXiv preprint arXiv:2312.11805 (2023) [2](#)
47. Thurstone, L.L.: A law of comparative judgment. Psychological Review **34**, 273–286 (1927) [6](#)
48. Topiwala, P., Dai, W., Pian, J., Biondi, K., Krovvidi, A.: VMAF and variants: Towards a unified VQA. In: Applications of Digital Image Processing. vol. 11842, pp. 96–104 (2021) [4](#)
49. Touvron, H., Lavril, T., Izacard, G., Martinet, X., Lachaux, M.A., Lacroix, T., Rozière, B., Goyal, N., Hambro, E., Azhar, F., et al.: LLaMA: Open and efficient foundation language models. arXiv preprint arXiv:2302.13971 (2023) [2](#)

50. Vaswani, A., Shazeer, N., Parmar, N., Uszkoreit, J., Jones, L., Gomez, A.N., Kaiser, L., Polosukhin, I.: Attention is all you need. In: *Advances in Neural Information Processing Systems*. vol. 30, pp. 5998–6008 (2017) [2](#)
51. Wang, Z., Xu, K., Yang, Y., Dong, J., Gu, S., Xu, L., Fang, Y., Ma, K.: Measuring perceptual color differences of smartphone photographs. *IEEE Transactions on Pattern Analysis and Machine Intelligence* **45**(8), 10114–10128 (2023) [4](#), [10](#)
52. Wang, Z., Bovik, A.C., Sheikh, H.R., Simoncelli, E.P.: Image quality assessment: From error visibility to structural similarity. *IEEE Transactions on Image Processing* **13**(4), 600–612 (2004) [2](#), [4](#), [13](#)
53. Wei, J., Bosma, M., Zhao, V.Y., Guu, K., Yu, A.W., Lester, B., Du, N., Dai, A.M., Le, Q.V.: Finetuned language models are zero-shot learners. In: *International Conference on Learning Representations* (2022) [2](#)
54. Wei, J., Wang, X., Schuurmans, D., Bosma, M., Xia, F., Chi, E., Le, Q.V., Zhou, D., et al.: Chain-of-thought prompting elicits reasoning in large language models. In: *Advances in Neural Information Processing Systems*. vol. 35, pp. 24824–24837 (2022) [8](#)
55. Wu, H., Zhang, Z., Zhang, E., Chen, C., Liao, L., Wang, A., Li, C., Sun, W., Yan, Q., Zhai, G., et al.: Q-Bench: A benchmark for general-purpose foundation models on low-level vision. In: *International Conference on Learning Representations* (2024) [3](#), [4](#)
56. Wu, H., Zhang, Z., Zhang, E., Chen, C., Liao, L., Wang, A., Xu, K., Li, C., Hou, J., Zhai, G., et al.: Q-Instruct: Improving low-level visual abilities for multi-modality foundation models. *arXiv preprint arXiv:2311.06783* (2023) [3](#), [4](#), [13](#), [14](#)
57. Wu, H., Zhang, Z., Zhang, W., Chen, C., Liao, L., Li, C., Gao, Y., Wang, A., Zhang, E., Sun, W., et al.: Q-Align: Teaching LMMs for visual scoring via discrete text-defined levels. *arXiv preprint arXiv:2312.17090* (2023) [3](#), [10](#)
58. Wu, H., Zhu, H., Zhang, Z., Zhang, E., Chen, C., Liao, L., Li, C., Wang, A., Sun, W., Yan, Q., et al.: Towards open-ended visual quality comparison. *arXiv preprint arXiv:2402.16641* (2024) [12](#)
59. Wu, T., Shi, S., Cai, H., Cao, M., Xiao, J., Zheng, Y., Yang, Y.: Assessor360: Multi-sequence network for blind omnidirectional image quality assessment. In: *Advances in Neural Information Processing Systems*. vol. 36, pp. 1–14 (2024) [4](#)
60. Yang, S., Wu, T., Shi, S., Lao, S., Gong, Y., Cao, M., Wang, J., Yang, Y.: MANIQA: Multi-dimension attention network for no-reference image quality assessment. In: *IEEE/CVF Conference on Computer Vision and Pattern Recognition Workshop*. pp. 1191–1200 (2022) [3](#), [4](#), [10](#), [13](#), [14](#)
61. Yang, Z., Li, L., Lin, K., Wang, J., Lin, C.C., Liu, Z., Wang, L.: The dawn of LMMs: Preliminary explorations with GPT-4V(ision). *arXiv preprint arXiv:2309.17421* (2023) [2](#), [4](#), [10](#), [11](#), [12](#), [13](#), [14](#), [15](#)
62. Ye, P., Doermann, D.: Active sampling for subjective image quality assessment. In: *IEEE/CVF Conference on Computer Vision and Pattern Recognition*. pp. 4249–4256 (2014) [6](#)
63. Ye, P., Kumar, J., Kang, L., Doermann, D.: Unsupervised feature learning framework for no-reference image quality assessment. In: *IEEE/CVF Conference on Computer Vision and Pattern Recognition*. pp. 1098–1105 (2012) [4](#)
64. Ye, Q., Xu, H., Ye, J., Yan, M., Liu, H., Qian, Q., Zhang, J., Huang, F., Zhou, J.: mPLUG-Owl2: Revolutionizing multi-modal large language model with modality collaboration. *arXiv preprint arXiv:2311.04257* (2023) [2](#), [3](#), [10](#), [11](#), [13](#), [14](#)
65. Yin, S., Fu, C., Zhao, S., Li, K., Sun, X., Xu, T., Chen, E.: A survey on multimodal large language models. *arXiv preprint arXiv:2306.13549* (2023) [8](#)

66. Ying, Z., Niu, H., Gupta, P., Mahajan, D., Ghadiyaram, D., Bovik, A.: From patches to pictures (PaQ-2-PiQ): Mapping the perceptual space of picture quality. In: IEEE/CVF Conference on Computer Vision and Pattern Recognition. pp. 3575–3585 (2020) [3](#)
67. You, Z., Li, Z., Gu, J., Yin, Z., Xue, T., Dong, C.: Depicting beyond scores: Advancing image quality assessment through multi-modal language models. arXiv preprint arXiv:2312.08962 (2023) [3](#), [4](#), [14](#)
68. Zhang, L., Zhang, L., Mou, X., Zhang, D.: FSIM: A feature similarity index for image quality assessment. IEEE Transactions on Image Processing **20**(8), 2378–2386 (2011) [13](#)
69. Zhang, R., Isola, P., Efros, A.A., Shechtman, E., Wang, O.: The unreasonable effectiveness of deep features as a perceptual metric. In: IEEE/CVF Conference on Computer Vision and Pattern Recognition. pp. 586–595 (2018) [3](#), [4](#), [10](#), [13](#)
70. Zhang, W., Ma, K., Zhai, G., Yang, X.: Uncertainty-aware blind image quality assessment in the laboratory and wild. IEEE Transactions on Image Processing **30**, 3474–3486 (2021) [4](#)
71. Zhang, W., Zhai, G., Wei, Y., Yang, X., Ma, K.: Blind image quality assessment via vision-language correspondence: A multitask learning perspective. In: IEEE/CVF Conference on Computer Vision and Pattern Recognition. pp. 14071–14081 (2023) [2](#), [3](#), [4](#), [10](#), [13](#), [14](#)
72. Zhu, D., Chen, J., Shen, X., Li, X., Elhoseiny, M.: MiniGPT-4: Enhancing vision-language understanding with advanced large language models. arXiv preprint arXiv:2304.10592 (2023) [4](#)
73. Zhu, H., Sui, X., Chen, B., Liu, X., Chen, P., Fang, Y., Wang, S.: 2AFC prompting of large multimodal models for image quality assessment. arXiv preprint arXiv:2402.01162 (2024) [3](#), [7](#)
74. Zhuang, S., Hadfield-Menell, D.: Consequences of misaligned AI. In: Advances in Neural Information Processing Systems. vol. 33, pp. 15763–15773 (2020) [8](#)